

Bandpass Filters Based SIW Square Cavity with Novel Feeding and Coupling Schemes

Bo Yin^{1, 2, *}, Qianqian Huang¹, and Xiangyu Shi¹

Abstract—This paper presents two novel different feeding and coupling schemes to solve the problem of generating transmission zeros (TZ) in lower stopband and their applications to design single-band filters. The designed two filters are based on substrate integrated waveguide (SIW) square cavity with orthogonal ports. In the design of Filter A, two L-shaped stubs are introduced to form an additional coupling path between two ports, which cause the generation of one TZ. Other two TZs are formed due to the resonance characteristics of L-shaped stubs and ports offset. Two metal vias are used to adjust center frequency slightly. In the design of Filter B, other two stubs are designed to form two additional coupling paths, thus forming a total of three coupling paths with the original path. Two TZs are obtained by utilizing the phase difference between different paths, and one TZ is generated for the resonance characteristics of the proposed stub 3. Simultaneously, an L-shaped slot is used to adjust center frequency. Both designed filters use the coplanar waveguide (CPW) structure to control bandwidth. Two filters are set to operate at 14.4 GHz with bandwidth of 800 MHz. Both filters are fabricated and measured. The simulation results of two filters are in good agreement with the measured ones.

1. INTRODUCTION

With the rapid development of modern wireless communication technology, increasing attention is paid for the devices operating in the microwave band [1]. As one of the significant radio frequency (RF) devices, microwave bandpass filters are widely researched in recent years. However, traditional metal waveguide filter is hardly integrated due to its large size. And microstrip filters have the disadvantage of high loss, which is further amplified at high frequency. So, the appearance of substrate integrated waveguide (SIW) greatly promotes the development of microwave filters. SIW combines advantages of metal waveguide and planar microstrip line, having been studied by scholars [2–5]. In [6], a bandpass filter with adjustable passbands is presented on SIW square resonant cavity. Multiple higher-order modes are utilized to generate passband, but the filter owns poor out-of-rejection due to the lack of transmission zeros (TZs). In [7], a bandpass filter with wide-stopband is reported. The wide-stopband performance is realized by the suppression of TE₁₀₂ mode. However, the filter considers only the TZ of upper stopband, not the lower stopband. The filter in [8] uses mixed quarter- and one-eighth modes to realize the miniaturization of structure, but it is similar to the filter in [7], not considering the TZ in lower stopband. In [9, 10], a complementary split ring resonator (CSRR) is used to design filters. In [9], although the introduction of CSRR widens bandwidth of the filter, it also increases the additional loss due to electromagnetic leakage. The filter in [10] ignores out-of-band performance, and its size is too large. In [11], electromagnetic bandgap structure (EBG), dual split ring resonator (DSRR), and

Received 29 April 2021, Accepted 10 June 2021, Scheduled 15 June 2021

* Corresponding author: Bo Yin (yinbo@cqupt.edu.cn).

¹ School of Optoelectronic Engineering, Chongqing University of Posts and Telecommunications, Chongqing 400065, China.

² Chongqing Municipal Level Key Laboratory of Photoelectronic Information Sensing and transmitting Technology, Chongqing 400065, China.

half-mode SIW technology are used to design filter, but these technologies do not improve the filter performance too much and make insertion loss poor. In [12], a miniaturized SIW filter is proposed. The miniaturization is obtained by half-mode principle and slow-wave technique. However, the filter has disadvantages of complex structure and bad out-of-rejection. A wide-stopband bandpass filter is reported in [13]. The wide-stopband performance is achieved by realizing the expected coupling of TE101 and TE102 modes of the cavity, but the out-of-band rejection of the low frequency is poor. A single-band bandpass filter using a single perturbed SIW circular cavity [14] is designed. Although it can realize the desired center frequency and bandwidth of passband by adjusting the metallic vias and slot perturbations, the filtering is poor due to the lack of TZs. In general, although SIW filters have been widely researched recently, not all the performance parameters are considered comprehensively. Besides, the research of transmission zero is mainly focused on microstrip filter [15–17]. For example, the TZ in lower stopband is rarely specially considered, which causes poor out-of-band rejection [18]. Therefore, it is necessary to design bandpass filters with TZs in lower stopband.

This article presents modified feeding and coupling schemes to generate TZs and their applications to design single-band filters. Two bandpass filters (Filter A and Filter B) with TZs on both sides are proposed. In the design of Filter A, the TZ in the upper stopband is generated by the orthogonal ports' offset, and the TZ in the low stopband is generated by another coupling path formed by an L-shaped stub. In the design of Filter B, two additional coupling paths are formed, which promotes the generation of TZs. Both filters are designed on Rogers RT/duriod 5880 substrate.

2. ANALYSIS AND DESIGN OF BANDPASS FILTERS

Three SIW square resonators with different feeding schemes are presented in Fig. 1. Fig. 1(a) depicts a SIW square resonator with orthogonal ports. The orthogonal ports excite the fundamental mode TE101, but the excitation is not enough to form a passband, which is verified in Fig. 2(a). Therefore, in order to form a passband, the coplanar waveguide structure (CPW) is introduced to SIW square cavity in Fig. 1(b). The combination of resonant frequency of the CPW structure and that of TE101 mode promotes the formation of the passband, which is verified in Fig. 2(b). Meanwhile, the modified orthogonal ports are presented in Fig. 1(c), which is off the center line. In the case of this offset, the coupling between CPW structures is affected with the decrease of distance between CPW structures. The direction of electric field has been changed, which leads to the formation of one TZ as shown in Fig. 2(c).

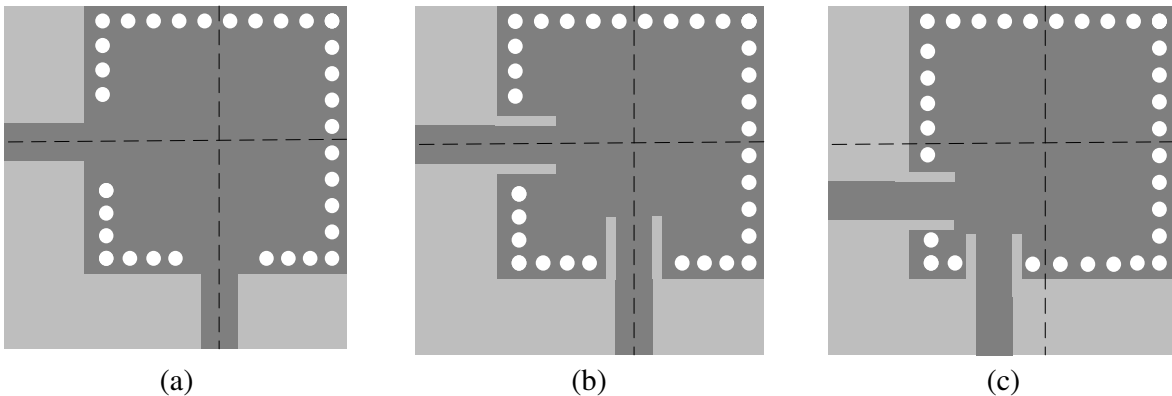


Figure 1. (a) The SIW square resonator with orthogonal ports. (b) The SIW square resonator with CPW structure and orthogonal ports. (c) The SIW square resonator with CPW structure and shifted orthogonal ports.

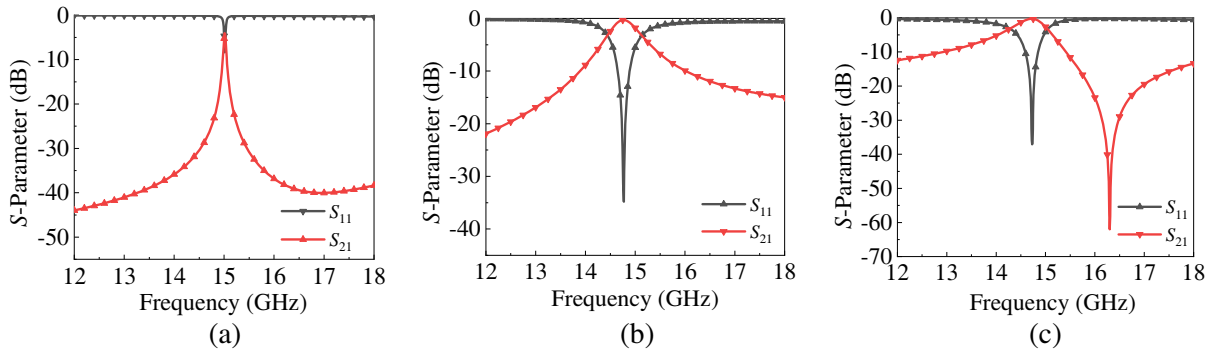


Figure 2. (a) S -parameters of the SIW square resonator with orthogonal ports. (b) S -parameters of the SIW square resonator with CPW structure and orthogonal ports. (c) S -parameters the SIW square resonator with CPW structure and shifted orthogonal ports.

2.1. The Design and Analysis of Filter A

Figure 3 illustrates the structure of proposed Filter A. Based on the structure in Fig. 1(c), two metal vias and two L-shaped stubs are introduced in Filter A. As perturbation elements, two metal vias are used to perturb electric field in SIW cavity, so as to adjust center frequency slightly. Simultaneously, an additional coupling path is created by loading two L-shaped stubs. The coupling scheme between two ports is shown in Fig. 4. There are two coupling paths between two ports. Path 1 is: Port 1→SIW cavity→Port 2. Path 2 is: Port 1→L-shaped 1→SIW cavity→L-shaped 2→Port 2. Fig. 5 depicts the comparison of S -parameters with and without L-shaped stubs. It can be found that three TZs are generated. Two TZs (TZ 1, TZ 2) are located in the lower stopband, and one TZ (TZ 3) is located in the upper stopband. TZ 1 is generated due to the resonance characteristics of L-shaped stubs. TZ 2 is generated by the phase difference between path 1 and path 2. TZ 3 is generated due to the offset of orthogonal ports. Therefore, the positions of TZ 1 and TZ 2 can be controlled by adjusting the dimensions of L-shaped stubs.

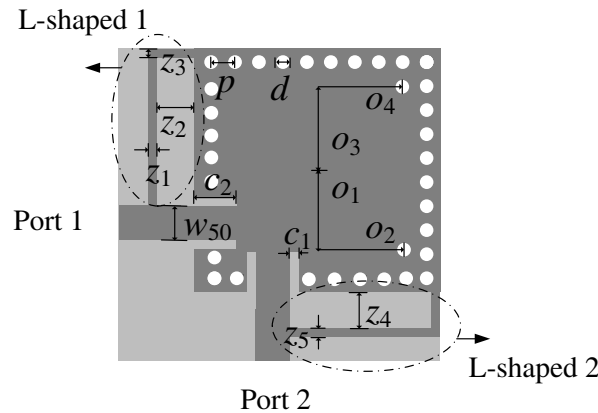


Figure 3. The structure diagram of proposed Filter A ($d = 0.6$ mm, $p = 1.1$ mm, $c_1 = 0.4$ mm, $c_2 = 1.8$ mm, $w_{50} = 1.2$ mm, $z_1 = 0.2$ mm, $z_2 = 1.6$ mm, $z_3 = 0.3$ mm, $z_4 = 1.6$ mm, $o_1 = 4$ mm, $o_2 = 4$ mm, $o_3 = 4$ mm, $o_4 = 4$ mm).

As depicted in Fig. 6, with the width of z_2 increasing from 1.1 mm to 1.5 mm, the location of TZ 2 is shifted towards high frequency, close to the passband, and the location of TZ 3 is hardly changed at all. That is because TZ 3 is generated due to the offset of orthogonal ports, independent of the L-shaped stubs. Simultaneously, as shown in Fig. 7, the locations of TZ 1 and TZ 2 can be adjusted by the width

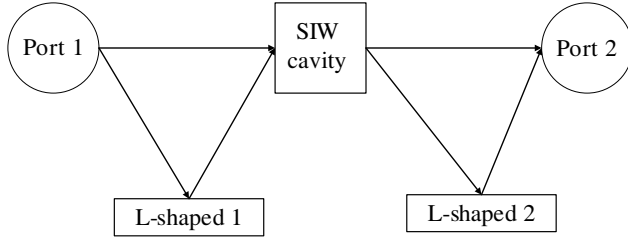


Figure 4. The coupling scheme between two ports in the Filter A.

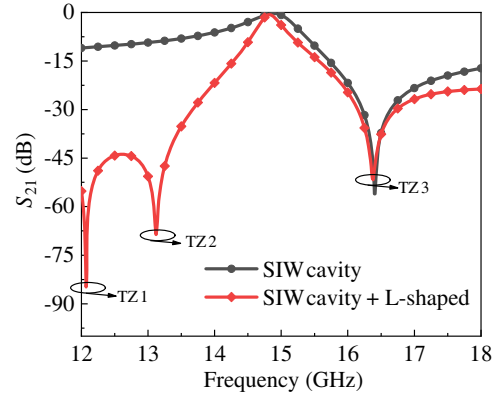


Figure 5. The S_{21} parameter of SIW cavity with and without L-shaped stubs.

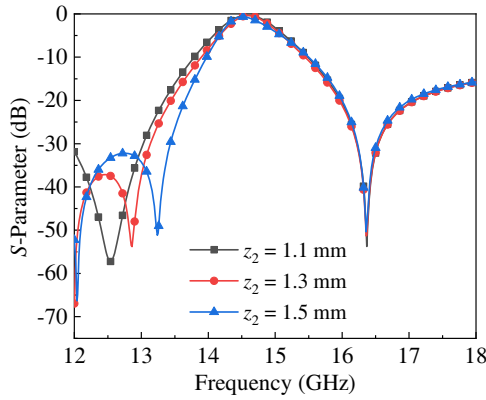


Figure 6. The S parameter with different width of z_2 .

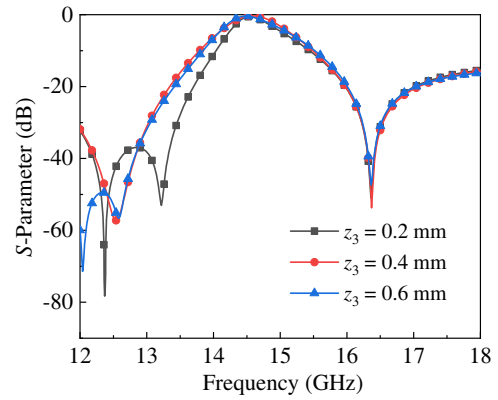


Figure 7. The S parameter with different width of z_3 .

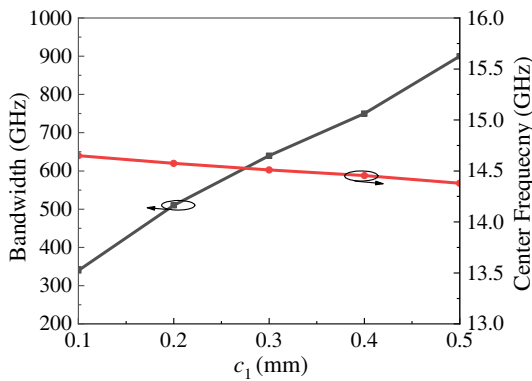


Figure 8. The bandwidths and center frequencies at different values of c_1 when c_2 is set to 1.8 mm.

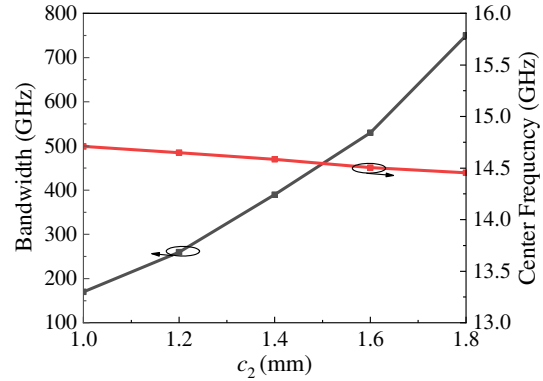


Figure 9. The bandwidths and center frequencies at different values of c_2 when c_1 is set to 0.4 mm.

of z_3 . TZ 1 and TZ 2 are closer to the passband as z_3 decreases from 0.4 mm to 0.2 mm. Therefore, the locations of TZ 1 and TZ 2 can be controlled by the reasonable specifications of L-shaped stubs.

On the other hand, bandwidth can be controlled flexibly by the CPW structure. In Fig. 8, as the width of c_1 increases from 0.1 mm to 0.5 mm when c_2 is set to 1.8 mm, bandwidth increases gradually, while center frequency is almost stable. As the length of c_2 increases from 1.0 mm to 1.8 mm when

c_1 is set to 0.4 mm, bandwidth also increases, and center is almost unchanged, which is depicted in Fig. 9. Therefore, Filter A has the ability to adjust bandwidth flexibly, and it can be applied to more applications.

2.2. The Design and Analysis of Filter B

Based on the SIW cavity in Fig. 1(b), Filter B is designed in Fig. 10. Similar to Filter A, the CPW structure is mainly used to generate passband and adjust bandwidth in the design of Filter B. In addition, an L-shaped slot is introduced to adjust center frequency. In order to improve the performance of filter better, three stubs are introduced to SIW cavity. Compared with Filter A, Filter B has some changes in the coupling scheme and the generations of TZs. From Fig. 11, it can be realized that there are three coupling paths between port 1 and port 2. Path 1 is: Port 1→SIW cavity→Port 2. Path 2 is: Port 1→stub 1→SIW cavity→stub 2→Port 2. Path 3 is: Port 1→stub 3→Port 2. As shown in Fig. 12, with the introduction of stub 1 and stub 2, the upper stopband performance of filter is improved, and the lower stopband performance of filter is improved with the introduction of stub 3. Three TZs are also obtained. TZ 1 is formed due to the phase difference between path 1 and path 3. TZ 2 is formed by the resonance characteristics of stub 3. TZ 3 is formed due to the phase difference between path 1 and path 2. Both TZ 1 and TZ 2 are related to stub 3, thus the positions of TZ 1 and TZ 2 can be controlled by adjusting the specification parameters of stub 3. The position of TZ 3 can be controlled by adjusting the specification parameters of stub 1 and stub 2. As shown in Fig. 13, the location of TZ 3 is changed at different widths of y_2 , while that of TZ 1 and TZ 2 is hardly affected, which proves that stubs 1, 2 mainly adjust TZ 3, and has little effect on TZ 1 and TZ 2. Therefore, TZ 1 and TZ 2 can be controlled by adjusting the specifications of stub 3, and TZ 3 can be controlled by adjusting the specifications of stub 1 and stub 2.

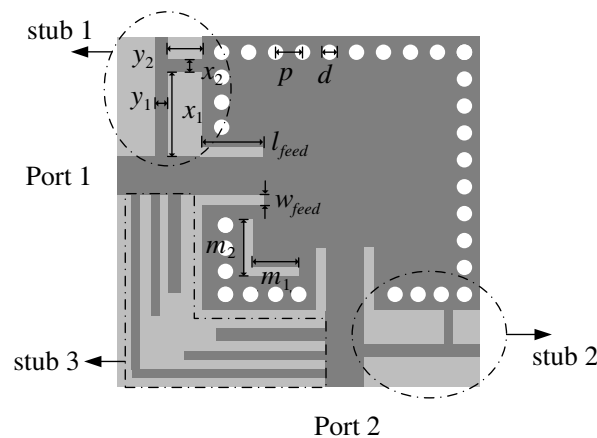


Figure 10. The structure diagram of proposed Filter B ($d = 0.7$ mm, $p = 1.1$ mm, $m_1 = 2.1$ mm, $m_2 = 2.3$ mm, $x_1 = 3.7$ mm, $x_2 = 0.2$ mm, $y_1 = 0.8$ mm, $y_2 = 1$ mm, $w_{feed} = 0.24$ mm, $l_{feed} = 2.9$ mm).

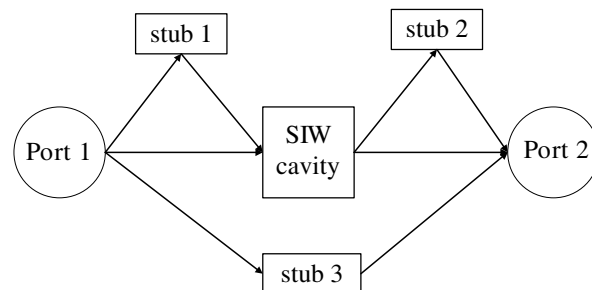


Figure 11. The coupling scheme between two ports in the Filter B.

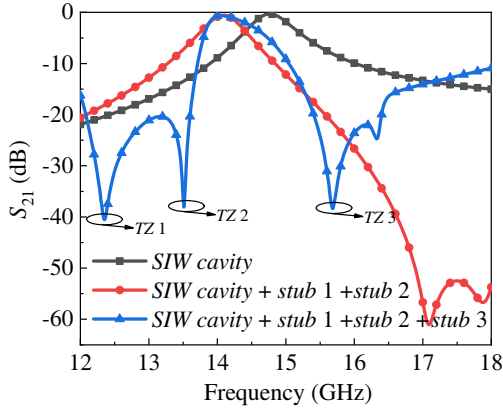


Figure 12. The S_{21} parameter of SIW cavity with and without stubs.

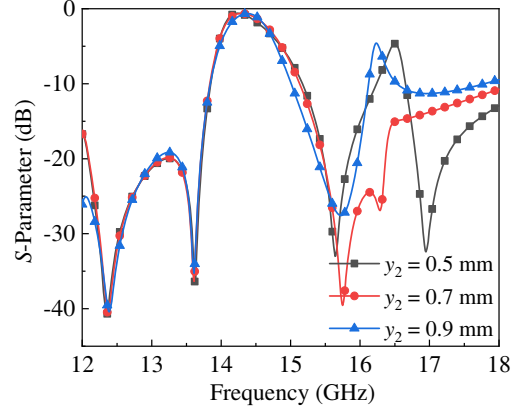


Figure 13. The S parameter with different width of y_2 .

3. THE ANALYSIS OF SIMULATION AND MEASUREMENT OF PROPOSED FILTER

In order to verify the feasibility of the designed coupling schemes, two filters are simulated, fabricated, and measured. Filter A and Filter B are set to operate at 14.4 GHz with bandwidth = 800 MHz. Fig. 14(a) shows a photo of the fabricated Filter A. Meanwhile, the simulated and measured results of Filter A are depicted in Fig. 15(a). The measured center frequency is at 14.39 GHz, and measured bandwidth is 820 MHz. The measured return loss is better than 12 dB. The minimum insertion loss is 1.45 dB. Three TZs are generated as expected. Fig. 14(b) shows a photo of the fabricated Filter B. Fig. 15(b) illustrates the simulation and measurement of Filter B, which operates at 14.35 GHz with bandwidth of 800 MHz. The measured return loss is better than 10 dB. The minimum insertion loss is 1.40 dB. Two phenomena can be found by comparing the simulation with the measurement. Phenomenon 1 is that center frequencies, bandwidths, return losses, and TZs remain almost unchanged. Phenomenon 2 is that insertion losses are deteriorated about 1 dB. But all the phenomena are within a reasonable range and can be explained. In the process of fabrication, the welding operation is manual, which may form errors and result in phenomenon 1. In addition, two filters are set to operate at high frequency band, so the loss of corresponding SMA connector cannot be ignored, which cause the appearance of phenomenon 2. On the whole, the simulated results of two filters are in good agreement with the measured ones. Table 1 shows the comparison between Filter A, B and other proposed filters. So, it can be concluded that the designed filters have merits of good out-of-band performance and compact structure.



(a)



(b)

Figure 14. (a) The photo of the fabricated Filter A; (b) The photo of the fabricated Filter B.

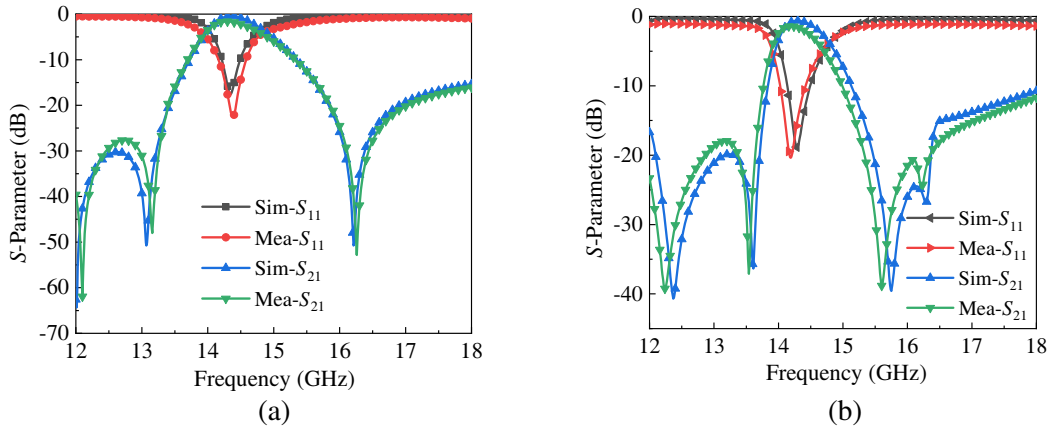


Figure 15. (a) The simulated and measured results of Filter A; (b) The simulated and measured results of Filter B.

Table 1. The comparison between Filter A, B and others proposed filters.

Ref	layers	CF (GHz)	IL (dB, @ f_0)	TZ _L	TZ _U	Size ($\lambda_g \times \lambda_g$)
[7]	1	9.97	1.65	0	2	1.47 * 0.77
[8]	1	8.00	0.90	0	1	0.43 * 0.27
[12]	1	12.65	2.50	0	0	0.35 * 1.17
[13]	1	10.04	1.50	0	1	0.48 * 1.06
[14]	1	7.43	1.80	0	0	0.65 * 0.65
[15]	4	6.96	2.29	0	1	0.46 * 0.46
Filter A	1	14.39	1.45	2	1	0.43 * 0.43
Filter B	1	14.35	1.40	2	1	0.48 * 0.48

4. CONCLUSION

In this paper, two different feeding and coupling schemes between two ports are presented. Based on SIW cavities with orthogonal ports, multiple coupling paths are formed by the introductions of multiple stubs between two ports, which solves the problem of generating TZs in the lower stopband. Three different stubs are designed. In addition, metal vias and L-shaped slots are used to adjust center frequency. The CPW structure is used to adjust bandwidth in both designed filters. Filter A and Filter B have advantages of good out-of-band performance and compact structure. The filters are in line with the development of microwave filters and suitable for satellite communication.

ACKNOWLEDGMENT

This work was supported by the National Natural Science Foundation of China (No: 61871063).

REFERENCES

- Deslandes, D. and K. Wu, "Single-substrate integration technique of planar circuits and waveguide filters," *IEEE Transactions on Microwave Theory and Techniques*, Vol. 51, No. 2, 593–596, Feb. 2003.

2. Liu, Y. J., G. Zhang, S. C. Liu, and J. Q. Yang, "Compact triple-band filter with adjustable passbands on one substrate integrated waveguide square resonant cavity," *Microwave and Optical Technology Letters*, Vol. 62, No. 12, 3709–3715, Jun. 2020.
3. Azad, A. R. and A. Mohan, "Compact bandpass filter with wide-stopband using substrate integrated waveguide cavities and short-circuited coplanar line," *International Journal of Microwave and Wireless Technologies*, Vol. 12, No. 5, 1–7, Jun. 2020.
4. Kim, P. and Y. Jeong, "Compact and wide stopband substrate integrated waveguide bandpass filter using mixed quarter- and one-eighth modes cavities," *IEEE Microwave and Wireless Components Letters*, Vol. 30, No. 1, 16–19, Jan. 2020.
5. Becharef, K., K. Nouri, H. Kandouci, B. S. Bouazza, M. Damou, and T. H. C. Bouazza, "Design and simulation of a broadband bandpass filter based on complementary split ring resonator circular "CSRRs"," *Wireless Personal Communications*, Vol. 111, No. 3, 1341–1354, Apr. 2020.
6. Moitra, S., S. Nayak, R. Regar, S. Kumari, K. Kumari, F. Parween, and F. Naseem, "Circular complementary split ring resonators (CSRR) based SIW BPF," *International Conference on Advanced Computational and Communication Paradigms, ICACCP*, 1–5, 2019.
7. Moitra, S. and P. S. Bhowmik, "Analyses of combined DSR and EBG structures over SIW and HMSIW for obtaining band pass response," *Wireless Personal Communications*, Vol. 111, No. 2, 1207–1218, Nov. 2019.
8. Khalil, M., M. Kamarei, and J. Jomaah, "Miniaturized half-mode slow-wave substrate-integrated waveguide bandpass filter," *Wireless Personal Communications*, Vol. 107, No. 1, 283–290, Jul. 2019.
9. Azad, A. R. and A. Mohan, "Substrate integrated waveguide dual-band and wide-stopband bandpass filters," *IEEE Microwave and Wireless Components Letters*, Vol. 28, No. 8, 660–662, Aug. 2018.
10. Azad, A. R. and A. Mohan, "Single- and dual-band bandpass filters using a single perturbed SIW circular cavity," *IEEE Microwave and Wireless Components Letters*, Vol. 29, No. 3, 201–203, Mar. 2019.
11. Zhang, H., W. Kang, and W. Wu, "Miniaturized dual-band SIW filters using E-shaped slotlines with controllable center frequencies," *IEEE Microwave and Wireless Components Letters*, Vol. 28, No. 4, 311–313, Apr. 2018.
12. Zhang, H., W. Kang, and W. Wu, "Dual-band substrate integrated waveguide bandpass filter utilising complementary split-ring resonators," *Electronic Letters*, Vol. 54, No. 2, 85–87, Jan. 2018.
13. Dong, Y., W. Hong, H. Tang, and W. Ke, "Millimeter-wave dual-mode filter using circular high-order mode cavities," *Microwave and Optical Technology Letters*, Vol. 51, No. 7, 1743–1745, Jul. 2009.
14. Chen, F., K. Song, B. Hu, and Y. Fan, "Compact dual-band bandpass filter using HMSIW resonator and slot perturbation," *IEEE Microwave and Wireless Components Letters*, Vol. 24, No. 10, 686–688, Oct. 2014.
15. Rebenaque, D., F. Pereira, J. Garcia, A. Melcon, and M. Guglielmi, "Two compact configurations for implementing transmission zeros in microstrip filters," *IEEE Microwave and Wireless Components Letters*, Vol. 14, No. 10, 475–477, Oct. 2004.
16. Mandal, M., K. Divyabramham, and V. Velidi, "Compact wideband bandstop filter with five transmission zeros," *IEEE Microwave and Wireless Components Letters*, Vol. 22, No. 1, 4–6, Jan. 2012.
17. Xu, K.-D., D. Li, and Y. Liu, "High-selectivity wideband bandpass filter using simple coupled lines with multiple transmission poles and zeros," *IEEE Microwave and Wireless Components Letters*, Vol. 29, No. 2, 107–109, Feb. 2019.
18. Lee, B., T.-H. Lee, K. Lee, M.-S. Uhm, and J. Lee, "K-band substrate-integrated waveguide resonator filter with suppressed higher-order mode," *IEEE Microwave and Wireless Components Letters*, Vol. 25, No. 6, 367–369, Jun. 2015.